DOI: 10.61782/fa.2023.0602

forum acusticum 2023

EXPERIMENTAL IMPLEMENTATION OF A FINITE-TIME CONTROLLER FOR THE AXISYMMETRIC VIBRATION MODES OF A TOM-TOM DRUM

Marc Wijnand[1*] **Brigitte d'Andréa-Novel**[1] **Thomas Hélie**[2] **David Roze**[2]
S3AM team, STMS lab (Ircam – [2]CNRS – [1]Sorbonne Université), Paris, France

ABSTRACT

This paper is concerned with the experimental implementation of a previously derived finite-time observer-regulator controlling the current of a loudspeaker mounted in a tom-tom drum, based on the measurement of its cavity pressure. The control goal is to modify frequency and damping of the axisymmetric vibration modes of the tom-tom membrane.

The first contribution constitutes the identification of the physical parameters of the tom-tom drum, such as membrane tension (from its observed Chladni figures) and viscous damping coefficient.

Secondly, the testbench for the controller evaluation is developed. It is shown how a reproducible excitation with a drumstick can be achieved. Then, the control law is implemented on a Coala microcontroller. A chattering phenomenon is observed, produced by the numerical stiffness of the control law, that can be removed by applying a regulatization by a local linearization close to the origin.

Finally, it is shown that the controller is able to modify frequencies of the axisymmetric vibration modes of the tom-tom membrane. However, there exists a disparity with respect to the frequency shifts predicted by the model used to tune the controller, that could be reduced by refining the model (in particular by taking into account the sound propagation inside the cavity).

Keywords: *musical acoustics, active control of musical instruments, finite-time control, experimental validation.*

1. INTRODUCTION

1.1 The tom-tom drum

The tom-tom drum is a directly struck membranophone. It consists of a cylindrical body with a top (*batter head*) and bottom (*resonant head*) membrane and is a standard part of a drum kit. The sound of the tom-tom drum is referred to as "indeterminately pitched" or "having a less clear pitch" [1]. The coupling between the air in the cavity and the (top) membrane improves the harmonicity of the axisymmetric vibration modes of the membrane [2], and increases the acoustical efficiency of the instrument [3].

1.2 Active control of musical instruments

Active control of musical instruments consists in adding a control loop to an existing acoustic musical instrument that is being played by a musician [4]. In terms of the actuator type, two classes of active vibration control are distinguished. In the case of *acoustical active control*, the control acts on a fluid medium. An example is the use of a loudspeaker to create destructive interference in order to cancel sound. In the case of *structural acoustical control*, the control acts on a solid. One can for example attach an actuator to the soundboard of a violin.

In most cases of active control of musical instruments, the goal is not to reduce vibrations as much as possible, but to change frequencies or damping coefficients of the instrument's vibration, enabling the musician to enlarge his sound palette while keeping the ergonomics of the original instrument. One can mention for instance applications to the (xylophone) beam [5], (clarinet) tube [6], (Chinese gong) metal plate [7] and (guitar) string [8].

Furthermore, active control of musical instruments can be invoked for the study of their dynamical behaviour [9], or for the removal of unwanted phenomena such as the so-called wolf note of the cello [10], or the bad playability of certain notes on the trombone when using a straight mute [11].

1.3 Active control of membranophones

Active control has been applied to following percussion instruments with a membrane-cavity coupling. In [12], control of four modes of a *drumhead* was obtained. A PID controller with stabilizing feedforward part was implemented, using four accelerometers on the drumhead as sensors and four loudspeakers acting

*__Corresponding author__: marc.wijnand@ircam.fr.

on the cavity as actuators. A *bass drum* [13] was controlled by a negative feedback, using a piezoceramic sensor attached to the rim to measure the membrane deflection and a single loudspeaker as actuator. A *conga* [14] was endowed with a contact microphone attached to the membrane as sensor and a single loudspeaker used as actuator enables to modify the instrument's frequency response. Feedback of a piezoelectric sensor placed on the batter head of a *tom-tom drum* [15] was applied on the resonant head by an electromagnetic actuator. A pickup dynamic microphone was placed inside an electromagnetic actuator placed on the batter head of a *bass drum* in [16]. Recently, a *snare drum* [17] was controlled using an optical sensor on the batter head, and multiple actuators: two tactile transducers on the resonant head, and an additional loudspeaker on a frame mounted inside the cavity.

Our contribution concerning the tom-tom drum focuses on the use of finite-time control methods [18], offering advantages regarding time constraints and robustness.

2. PREVIOUS RESULTS

The model and controller obtained in [19, 20] are restated here.

2.1 Model

2.1.1 PDE-ODE model

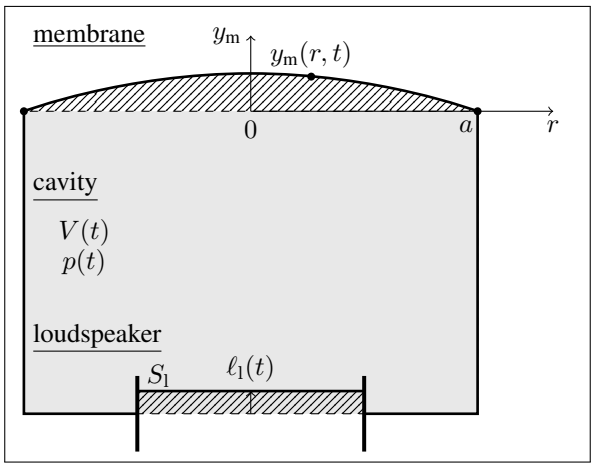

Figure 1: Geometry of the system

Following coupled PDE-ODE model for the system shown in Fig. 1 was obtained:

$$\begin{cases} T\boldsymbol{\Delta} y_\mathrm{m}(r,t) + p_\mathrm{c}(t) = \sigma_\mathrm{m}\dfrac{\partial^2}{\partial t^2} y_\mathrm{m}(r,t) + \mu\dfrac{\partial}{\partial t} y_\mathrm{m}(r,t) \\ p_\mathrm{c}(t) = -\gamma\dfrac{p_0}{V_0}\left[\displaystyle\int_{\mathcal{S}} y_\mathrm{m}(r,t)\,\mathrm{d}\mathcal{S}(r) - S_\mathrm{l}\ell_\mathrm{l}(t)\right] \\ m_\mathrm{l}\ddot{\ell}_\mathrm{l}(t) + c_\mathrm{l}\dot{\ell}_\mathrm{l}(t) + k_\mathrm{l}\ell_\mathrm{l}(t) = S_\mathrm{l}p_\mathrm{c}(t) + Bli_\mathrm{l}(t). \end{cases} \quad (1)$$

This model describes the evolutions of the transverse displacement of the tom-tom membrane $y_\mathrm{m}(r,t)$, the net pressure in the cavity $p_\mathrm{c}(t)$ and the transverse position of the loudspeaker membrane $\ell_\mathrm{l}(t)$.

The membrane is clamped at its rim: $y_\mathrm{m}(a,t) = 0$. The surface of the membrane $\mathcal{S}$ is defined between $r = 0$ and $r = a$, and $\boldsymbol{\Delta} = \frac{\partial^2}{\partial r^2} + \frac{1}{r}\frac{\partial}{\partial r}$ in polar coordinates. The physical constants of the membrane are its tension T, equivalent areal density $\sigma_\mathrm{m} = \sigma + 0.85a\rho_\mathrm{air}$ (with σ the real areal density, a the membrane's radius and ρ_air the volumetric density of air, [21]), and friction coefficient μ. The physical constants of the cavity are the heat capacity ratio of air γ and its pressure p_0 and volume V_0 at rest, that relate the net values $(p_\mathrm{c}, V_\mathrm{c})$ to the total values (p, V):

$$\begin{cases} p_\mathrm{c}(t) = p(t) - p_0 \\ V_\mathrm{c}(t) = V(t) - V_0. \end{cases}$$

The physical constants of the loudspeaker are its surface S_l, the Lorentz force factor Bl (with the length of the loudspeaker coil l inside the magnetic field B), and equivalent mass m_l, damper c_l and spring k_l.

2.1.2 ODE model

The model (1) was discretized by a modal projection and truncation:

$$y_\mathrm{m}(r,t) \approx \sum_{n=1}^{N} \varphi_n(r) z_n(t),$$

where $z_n(t)$ are the temporal evolutions corresponding to the respective N eigenfunctions

$$\varphi_n(r) = w_n\left[J_0(\lambda_n r) - J_0(\lambda_n a)\right]$$

with $J_0(\cdot)$ the Bessel function of the first kind of order 0, the wave numbers λ_n solutions of the implicit condition [19, Eq. 8] and w_n arbitrary weights.

2.2 Control

A controller for the loudspeaker current was designed, to let its membrane position (and thus the pressure inside the cavity) track a reference that realizes a pole placement on the tom-tom membrane. Thus, a modal control of frequencies and/or damping coefficients of the tom-tom membrane is possible.

The finite-time control law reads

$$\begin{aligned} i_\mathrm{l} = \frac{1}{Bl}\Big[& S_\mathrm{l}p_\mathrm{c}^\mathrm{m} + k_\mathrm{l}\ell_\mathrm{l}^\mathrm{m} + c_\mathrm{l}\dot{\ell}_\mathrm{l}^\mathrm{m} - k_3\left(\ell_\mathrm{l}^\mathrm{m} - \ell_\mathrm{l}^*\right) \\ & -k_4\left(\dot{\ell}_\mathrm{l}^\mathrm{m} - \dot{\ell}_\mathrm{l}^*\right) - k_1\left\lfloor \ell_\mathrm{l}^\mathrm{m} - \ell_\mathrm{l}^*\right\rceil^{\frac{\alpha}{2-\alpha}} - k_2\left\lfloor \dot{\ell}_\mathrm{l}^\mathrm{m} - \dot{\ell}_\mathrm{l}^*\right\rceil^{\alpha}\Big] \end{aligned} \quad (2)$$

with control parameters $k_1, k_2 > 0$, $\alpha \in \,]0,1[$ (to be tuned in simulation [20]), $k_3 > k_\mathrm{l}$, $k_4 > c_\mathrm{l}$, and $\lfloor x\rceil^\xi \triangleq \mathrm{sgn}(x)|x|^\xi$.

Here, the following signals are defined. The real pressure $p_\mathrm{c}^\mathrm{m}(t)$ is measured by a sensor. The reference pressure

$$p_\mathrm{c}^*(t) \triangleq -\sum_{i=1}^{N}\left[k_{i,a}z_i(t) + k_{i,b}\dot{z}_i(t)\right]$$

where coefficients $k_{i,a}$ and $k_{i,b}$ realizing the pole placement are designed in simulation [20]. The temporal evolutions $z_i(t)$ of the first N membrane modes are estimated by a finite-time observer obtained in [20, Lemma 2]. Lastly, the real (resp. reference) loudspeaker position $\ell_{\mathrm{l}}^{\mathrm{m}}(t)$ (resp. $\ell_{\mathrm{l}}^{*}(t)$) can be expressed as function of the real (resp. reference) pressure $p_{\mathrm{c}}^{\mathrm{m}}(t)$ (resp. $p_{\mathrm{c}}^{\mathrm{m}}(t)$), and $z_i(t)$ using relation [20, Eq. 13]; and similarly for their time derivatives.

3. IDENTIFICATION

Table 1 lists the physical parameters of the model that have to be identified in order to be able to calculate the control law (2). The used identification methods are mentioned below. More information and figures can be found in [22, Chapter 10].

Table 1: List of identified physical parameters

membrane	a	radius	0.162	m
	σ	mass density	0.267	$\frac{\mathrm{kg}}{\mathrm{m}^2}$
	T	tension	420	$\frac{\mathrm{N}}{\mathrm{m}}$
	μ	viscosity coefficient	1.4707	$\frac{\mathrm{l}}{\mathrm{s}}$
cavity	V_0	volume at rest	0.0195	m^3
loudspeaker	m_{l}	equivalent mass	0.157	kg
	c_{l}	equivalent damping	4.87	$\frac{\mathrm{kg}}{\mathrm{s}}$
	k_{l}	equivalent stiffness	7.80	$\frac{\mathrm{N}}{\mathrm{m}}$
	Bl	Lorentz force factor	17.4	$\mathrm{T}\cdot\mathrm{m}$
	R	electrical resistance	5.52	Ω
	L	electrical inductance	4.37	H
	S_{l}	equivalent surface	0.0515	m^2

3.1 Cavity

- The volume V_0 of the cavity at rest is obtained geometrically

3.2 Loudspeaker

A loudspeaker with nominal exterior diameter of 320 mm by Raveland (AXX 1212, US) is mounted.

- The equivalent surface S_{l} of the membrane is obtained geometrically.
- The listed Thiele & Small parameters are obtained by curve fitting the transfer function of the linear model to a measurement of voltage, current and displacement of the membrane when the loudspeaker is driven with a sine sweep voltage signal [23].

3.3 Membrane

A membrane with nominal diameter of 13" and *10-mil* thickness by Remo Inc. (US) is mounted on the circular edge of the tom. The membrane is tuned by trying to let frequencies around 100 Hz of split versions of the first observed mode (11) coincide (*clearing the membrane*, [24]). In this fashion, a (low) membrane tension is obtained, that is supposed to be as uniform as possible.

- The effective radius a is obtained geometrically.
- The surface mass density σ is obtained by weighing. A similar value of $0.262\,\mathrm{kg/m^2}$ was found in the same fashion for a timpani membrane in [25].
- The membrane tension is estimated from the Chladni figures (Fig. 2) that are visualized by exciting the membrane at a given frequency using the mounted loudspeaker or a shaker.

  Following the method proposed in [26], by fitting the theoretical frequencies of the non-axisymmetric eigenmodes (that depend on the tension) to the observed frequency ranges for the Chladni figures, the tension can be estimated (Fig. 3). Only modes 11 and 21 were considered here.

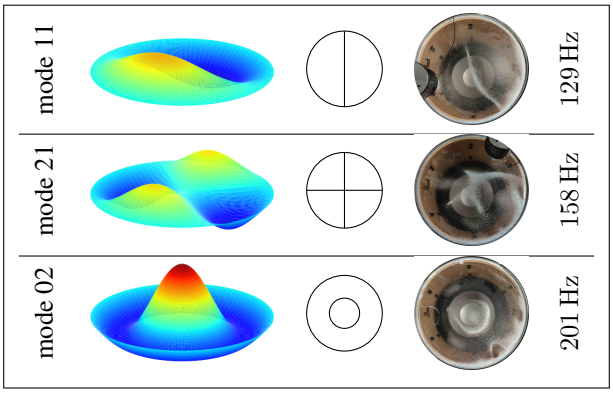

Figure 2: Some obtained Chladni figures

- The viscosity coefficient was estimated by the ESPRIT analysis method [27, 28] applied to the sound of the membrane after removing a slight pitch-glide (nonlinear) phenomenon. This method fits an EDS (Exponentially Damped Sinusoids) model to the time evolution of the pressure signal (Fig. 4).

4. TESTBENCH

4.1 Components

The total setup is shown in Fig. 5.

- Sensor: the microphone used to measure the pressure inside the cavity $p_{\mathrm{c}}(t)$ is introduced through a vent hole of the drum.
- Actuator: the control law for the current (2) is converted for the voltage-controlled loudspeaker by neglecting its

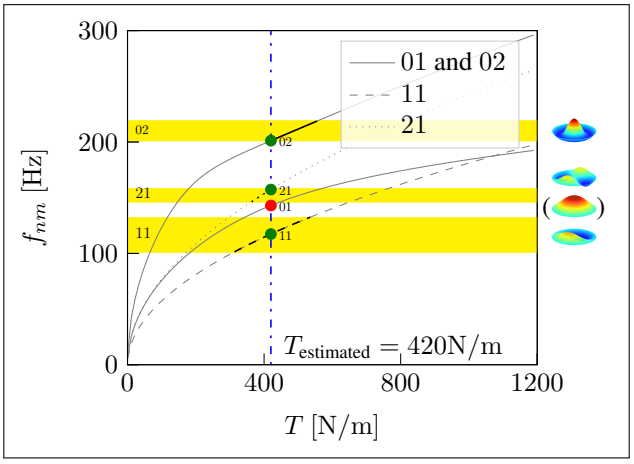

Figure 3: Fit of the frequencies of the model (indicated in gray as function of the unknown tension T) to the observed frequency ranges of the Chladni figures for modes $nm = 11, 21, 02$ (yellow zones).

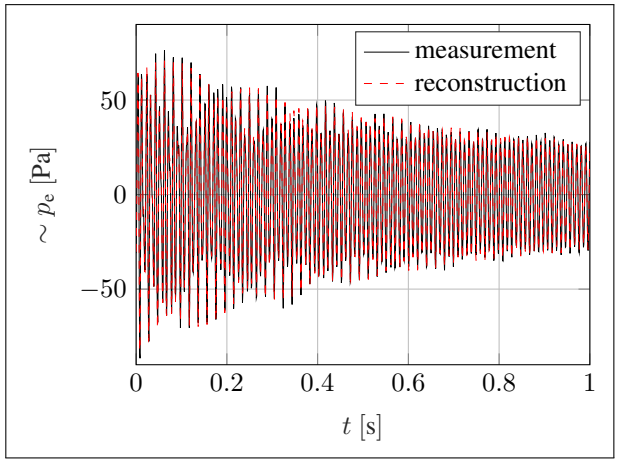

Figure 4: Approximation of the measured external pressure $p_e(t)$ by an EDS model with 4 pole pairs by the ESPRIT method

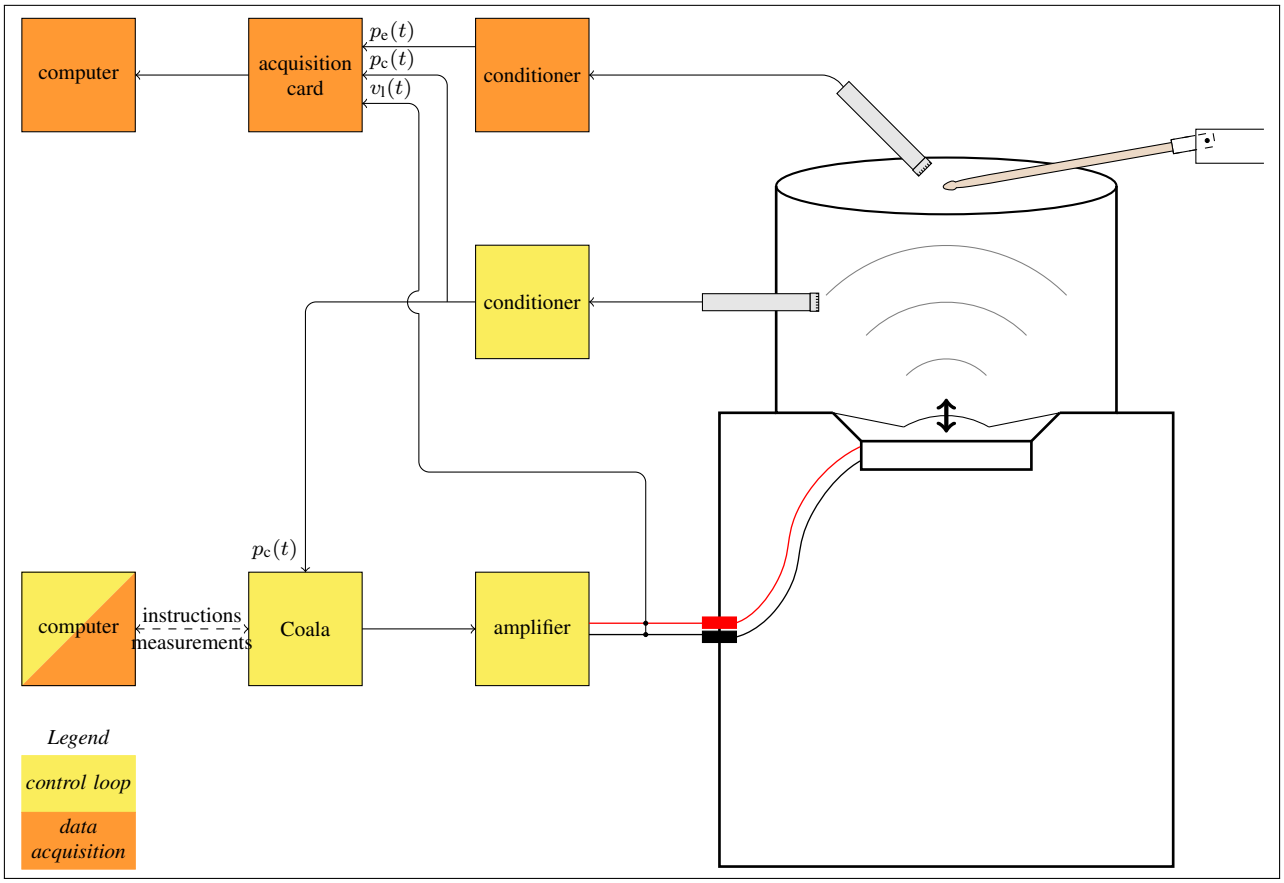

Figure 5: Total setup with a microphone as sensor, Coala as microcontroller and loudspeaker as actuator. The second microphone above the tom-tom drum is used to measure the external pressure $p_e(t)$.

inductance following

$$v_\mathrm{l}(t) = Ri_\mathrm{l}(t) + L\cancel{\frac{\mathrm{d}i_\mathrm{l}(t)}{\mathrm{d}t}} + Bl\dot{\ell}_\mathrm{l}(t).$$

- Controller: the control law for $N = 2$ modes is discretized by Euler's explicit method and implemented on a Coala microcontroller, suited for single-input-single-output control with a latency lower than 100 µs [29].

4.2 Reproducible excitation mechanism

A reproducible excitation mechanism is built by mounting a drumstick in a hinge (Fig. 6(a)). Releasing the drumstick that is initially held against a stop and catching it after one impact, enables to obtain a repeatable force in magnitude and impact point, as shown in Fig. 6(b).

5. EVALUATION

5.1 Numerical stiffness

When testing the control loop, a high-frequency noise is noticed (Fig. 7), even when the pressure inside the cavity is very small. This chattering phenomenon is caused by the inherent stiffness [18] of the nonlinear expression $\lfloor x \rceil^\xi$ in the used finite-time control law (2) at $x = 0$. A local linearization [1] of these expressions around 0 suffices to remove this phenomenon (Fig. 7).

[1] The (nondimensionalized [19, 20]) arguments x of $\lfloor x \rceil^\xi$ in the expression of the observer (resp. controller) were linearized in an interval $[-10^{-5}, 10^{-5}]$ (resp. $[-10^{-3}, 10^{-3}]$).

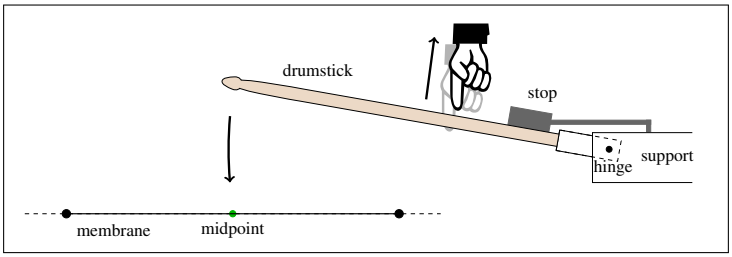

(a) Principle

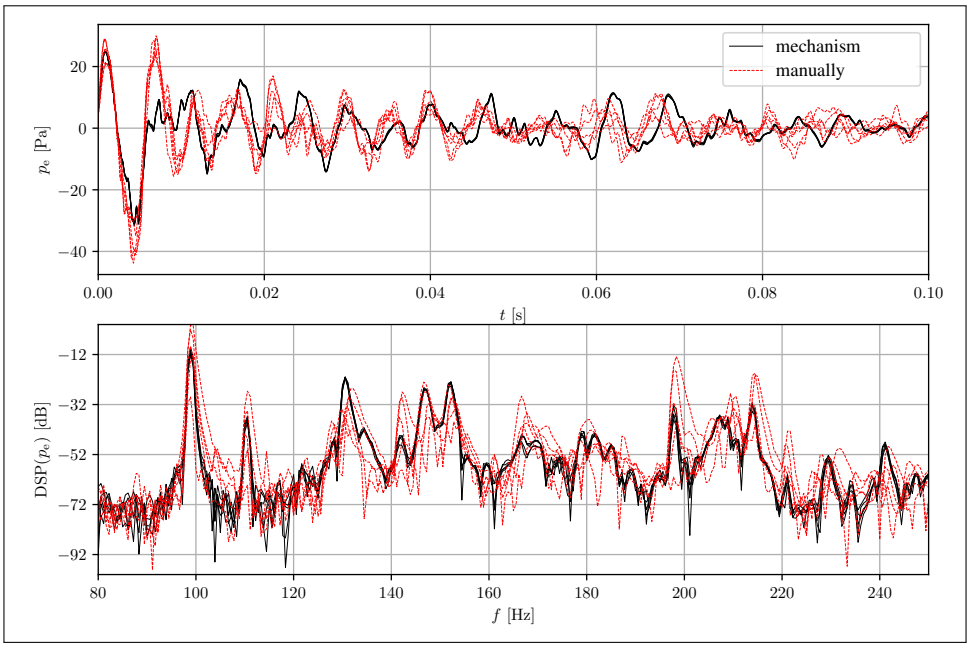

(b) Efficiency evaluated by comparing time and frequency evolutions for 5 manual impacts vs. 5 impacts with the excitation mechanism: the temporal measurements coincide almost perfectly in the latter case.

Figure 6: Reproducible excitation mechanism

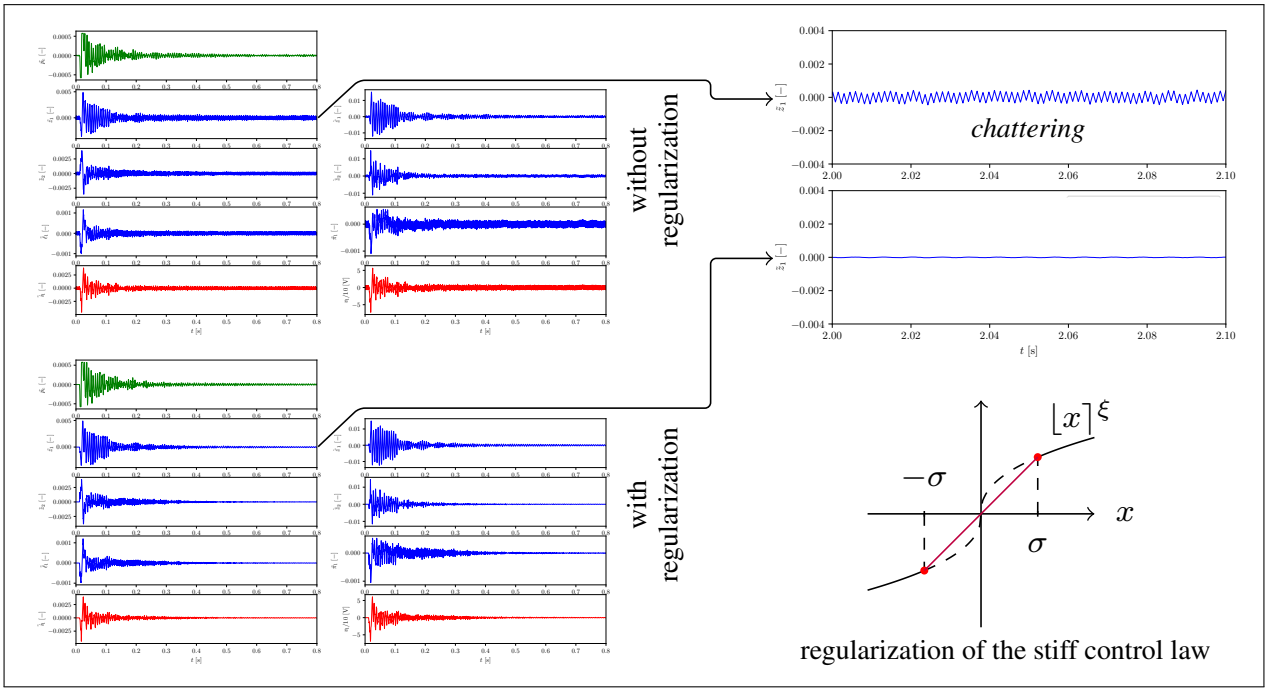

Figure 7: Evaluation of the numerical method. The internal variables of the Coala are depicted: pressure measurement in green, state of the observer in blue ($N = 2$ modes and loudspeaker), calculated current/tension control law in red. They exhibit a chattering phenomenon (the case of $\tilde{z}_1(t)$ being shown well after an impact), that is removed by a regularization of the expression $\lfloor x \rceil^{\xi}$. (Tildes indicate nondimensionalized versions of the respective signals, cf. [19, 20].)

5.2 Frequency change

The testbench is placed in Ircam's anechoic chamber. Different sets of pole placement parameters $(k_{i,a}, k_{i,b})$ are selected and for each, the resulting sound is measured thrice (Fig. 8). It is shown that the controller enables to obtain frequency shifts. However, differences with the frequency shifts predicted in simulation are observed (and the measured spectrum is more complex than the simulated spectrum).

6. CONCLUSION AND PERSPECTIVES

The experimental implementation of a previously derived finite-time observer-regulator for a tom-tom drum augmented with a loudspeaker was discussed.

Firstly, a chattering phenomenon was observed, caused by the stiffness of the used control law. This was removed by a local linearization of the control law.

Secondly, it was shown that the proposed control architecture enables to modify frequencies of the tom-tom membrane, while sensor and actuator are located outside the membrane domain. However, differences have been observed between the measured frequency shifts and those predicted by the simulation used while tuning the control parameters.

In order to improve the performance of the proposed finite-time observer-regulator structure, the used model could be refined. The most important contribution would be to include the neglected time delays that exist between sensor, membrane and actuator. Furthermore, the cavity and radiation dynamics could be included, and the tuning of the membrane studied more thoroughly.

7. ACKNOWLEDGMENTS

Brigitte d'Andréa-Novel and Marc Wijnand were supported by ANR project Finite4SoS (ANR 15 CE23 0007). The authors thank Emmanuel Fléty, Tristan Lebrun, Robert Piéchaud and Arnaud Recher for technical support.

8. REFERENCES

[1] S. Z. Solomon, *How to write for Percussion: a comprehensive guide to percussion composition*. Oxford University Press, 2016.

[2] R. S. Christian, R. E. Davis, A. Tubis, C. A. Anderson, R. I. Mills, and T. D. Rossing, "Effects of air loading on timpani

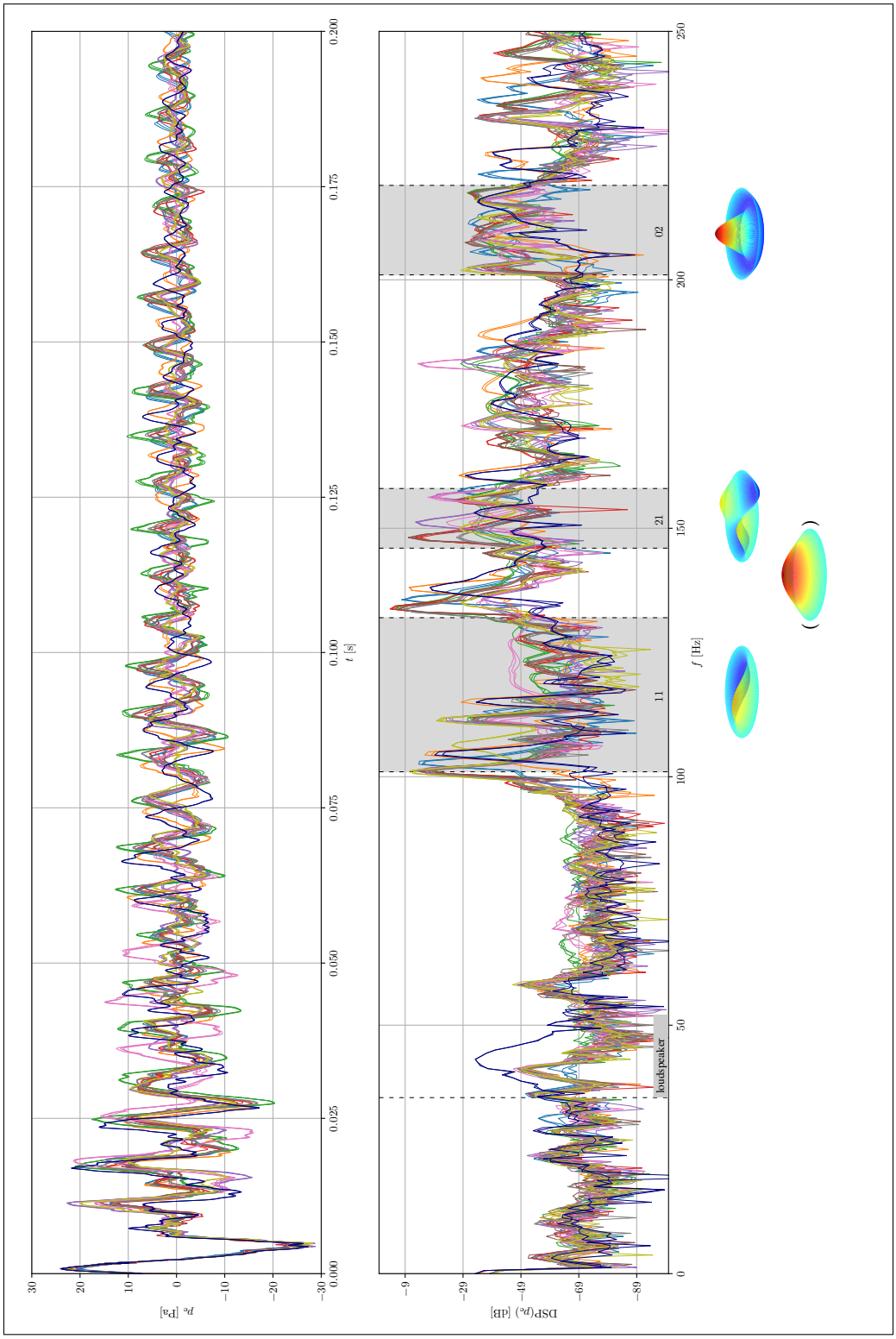

Figure 8: Power spectral density for measurements of the pressure $p_e(t)$ obtained with different pole placement parameters (different colours). The uncontrolled case is indicated in black; and frequency bands for the experimentally observed Chladni figures are indicated in gray.

membrane vibrations," *The Journal of the Acoustical Society of America*, vol. 76, no. 5, pp. 1336–1345, 1984.

[3] A. Chaigne and J. Kergomard, *Acoustics of musical instruments*. Springer, 2016.

[4] C. Besnainou, "Comment changer la voix des instruments de musique," *Rencontres Musicales Pluridisciplinaires, GRAME, Lyon*, 2006.

[5] H. Boutin, C. Besnainou, and J.-D. Polack, "Modifying the resonances of a xylophone bar using active control," *Acta Acustica united with Acustica*, vol. 101, no. 2, pp. 408–420, 2015.

[6] T. Meurisse, A. Mamou-Mani, S. Benacchio, B. Chomette, V. Finel, D. B. Sharp, and R. Caussé, "Experimental Demonstration of the Modification of the Resonances of a Simplified Self-Sustained Wind Instrument Through Modal Active Control," *Acta Acustica united with Acustica*, vol. 101, no. 3, pp. 581–593, 2015.

[7] M. Jossic, A. Mamou-Mani, B. Chomette, D. Roze, F. Ollivier, and C. Josserand, "Modal active control of Chinese gongs," *The Journal of the Acoustical Society of America*, vol. 141, no. 6, pp. 4567–4578, 2017.

[8] M. Wijnand, T. Hélie, and D. Roze, "Finite-time tracking control of a nonlinear string to reference dynamics," in *10th European Nonlinear Dynamics Conference (ENOC)*, 2022.

[9] S. Benacchio, A. Mamou-Mani, B. Chomette, and V. Finel, "Active control and sound synthesis–two different ways to investigate the influence of the modal parameters of a guitar on its sound," *The Journal of the Acoustical Society of America*, vol. 139, no. 3, pp. 1411–1419, 2016.

[10] P. Neubauer, J. Tschesche, J. Bös, T. Melz, and H. Hanselka, "An active-system approach for eliminating the wolf note on a cello," *The Journal of the Acoustical Society of America*, vol. 143, no. 5, pp. 2965–2974, 2018.

[11] T. Meurisse, A. Mamou-Mani, R. Caussé, B. Sluchin, and D. B. Sharp, "An active mute for the trombone," *The Journal of the Acoustical Society of America*, vol. 138, no. 6, pp. 3539–3548, 2015.

[12] J. D. T. Rollow IV, *Active Control of Spectral Detail Radiated by an air-loaded impacted membrane*. PhD thesis, The Pennsylvania State University, 2003.

[13] M. Lupone and L. Seno, "Gran cassa and the adaptive instrument feed-drum," in *International Symp. on Computer Music Modeling and Retrieval*, pp. 149–163, Springer, 2005.

[14] M. Van Walstijn and P. Rebelo, "The prosthetic conga: Towards an actively controlled hybrid musical instrument," in *ICMC*, Citeseer, 2005.

[15] J. Gregorio and Y. Kim, "Augmentation of acoustic drums using electromagnetic actuation and wireless control," *Journal of the Audio Engineering Society*, vol. 66, no. 4, pp. 202–210, 2018.

[16] D. Rector and S. Topel, "EMdrum: An Electromagnetically Actuated Drum," in *Proc. of NIME*, pp. 395–398, 2014.

[17] P. Williams and D. Overholt, "Design and evaluation of a digitally active drum," *Personal and Ubiquitous Computing*, 2020.

[18] S. P. Bhat and D. S. Bernstein, "Finite-time stability of continuous autonomous systems," *SIAM Journal on Control and Optimization*, vol. 38, no. 3, pp. 751–766, 2000.

[19] M. Wijnand, B. d'Andréa-Novel, B. Fabre, T. Hélie, L. Rosier, and D. Roze, "Active control of the axisymmetric vibration modes of a tom-tom drum," in *2019 IEEE 58th Conference on Decision and Control (CDC)*, IEEE, 2019.

[20] M. Wijnand, B. d'Andréa-Novel, T. Hélie, and D. Roze, "Active control of the axisymmetric vibration modes of a tom-tom drum using a modal-based observer-regulator," in *EAA e-Forum Acusticum*, 2020.

[21] L. E. Kinsler, A. R. Frey, A. B. Coppens, and J. V. Sanders, *Fundamentals of acoustics*. Wiley, 1999 (4th edition).

[22] M. Wijnand, *Contrôle en temps fini de systèmes vibratoires hybrides couplant équations aux dérivées partielles et équations aux dérivées ordinaires : les cas du tom et du câble pesant*. PhD thesis, Sorbonne Université, Paris, France, 2021.

[23] T. Lebrun, *Modélisation multi-physique passive, identification, simulation, correction et asservissement de haut-parleur sur des comportements cibles*. PhD thesis, 2019.

[24] P. G. M. Richardson and E. R. Toulson, "Clearing the drumhead by acoustic analysis method," in *Proceedings of the Institute on Acoustics, Reproduced Sound Conference, Cardiff, Wales, UK*, 2010.

[25] L. Rhaouti, A. Chaigne, and P. Joly, "Time-domain modeling and numerical simulation of a kettledrum," *The Journal of the Acoustical Society of America*, vol. 105, no. 6, pp. 3545–3562, 1999.

[26] A. Chaigne, "Détermination expérimentale de la tension d'une peau de timbale," in *Actes du 5ème Congrès Français d'Acoustique*, pp. 251–253, 2000.

[27] R. Roy, A. Paulraj, and T. Kailath, "ESPRIT–A subspace rotation approach to estimation of parameters of cisoids in noise," *IEEE transactions on acoustics, speech, and signal processing*, vol. 34, no. 5, pp. 1340–1342, 1986.

[28] M. Lagrange, R. Badeau, B. David, N. Bertin, J. Echeveste, O. Derrien, S. Marchand, and L. Daudet, "The desam toolbox: spectral analysis of musical audio," in *International Conference on Digital Audio Effects (DAFx), Graz*, 2010.

[29] R. Piéchaud, "A lightweight C++ framework for real time active control," in *Real time Linux workshop*, 2014.